Polarizable Continuum Model (PCM) Calculations of Solvent Effects on Optical Rotations of Chiral Molecules

B. Mennucci*,† and J. Tomasi

Dipartimento di Chimica e Chimica Industriale, Università di Pisa, Via Risorgimento 35, 56126 Pisa, Italy

R. Cammi

Dipartimento di Chimica Generale ed Inorganica, Università di Parma, Parco Area delle Scienze 1, 43100 Parma, Italy

J. R. Cheeseman*,‡ and M. J. Frisch

Gaussian Inc., 140 Washington Avenue, North Haven, Connecticut 06473

F. J. Devlin, S. Gabriel, and P. J. Stephens*,§

Department of Chemistry, University of Southern California, Los Angeles, California 90089-0482

Received: January 16, 2002; In Final Form: March 19, 2002

A new theory of solvent effects on the optical rotations of chiral molecules is presented. The frequency-dependent electric dipole−magnetic dipole polarizability, $\beta_{\alpha\beta}(\nu)$, is calculated using density functional theory (DFT). Solvent effects are included using the polarizable continuum model (PCM). DFT/PCM calculations of sodium D line specific rotations, $[\alpha]_D$, have been carried out for seven conformationally rigid chiral organic molecules (fenchone, camphor, α-pinene, β-pinene, camphorquinone, verbenone, and methyloxirane) for a diverse set of seven solvents (cyclohexane, carbon tetrachloride, benzene, chloroform, acetone, methanol, and acetonitrile). The predicted variation in $[\alpha]_D$ for the solvents cyclohexane, acetone, methanol, and acetonitrile are in excellent agreement with experiment for all seven molecules. For the solvents carbon tetrachloride, benzene, and chloroform, agreement is much poorer. Since only electrostatic solute−solvent interactions are included in the PCM, our results lead to the conclusion that, for the seven molecules studied, in cyclohexane, acetone, methanol, and acetonitrile electrostatic effects are dominant while in carbon tetrachloride, benzene, and chloroform other nonelectrostatic effects are more important. The observed variations in $[\alpha]_D$ with solvent are inconsistent, both qualitatively and quantitatively, with the variations predicted by the equation $[\alpha]_D(\text{solvent}) = \{[\alpha]_D(\text{gas})\}(n_D^2 + 2)/3$.

Introduction

Chiral molecules exhibit optical rotation. With very few exceptions, optical rotation measurements are carried out in the condensed phase, most often in liquid solutions. Optical rotations of solutions of chiral molecules are solvent-dependent.[1] In the case of flexible molecules, which exhibit multiple conformations in solution, solvent effects can often be attributed predominantly to changes in conformational populations with solvent. However, in the case of rigid molecules exhibiting a single conformation, optical rotations can still exhibit substantial solvent dependence. For example, $[\alpha]_D$ for (+)-methyloxirane varies from +30.6° to −4.3° over a range of 35 solvents.[2]

In this paper, we present a new theory of solvent effects on optical rotations. Optical rotations are calculated using density functional theory (DFT).[3] Solvent effects are incorporated using the integral equation formalism (IEF)[4] version of the polarizable continuum model (PCM).[5] The accuracy of the DFT/PCM theory is evaluated by comparison of its predictions for seven conformationally rigid chiral organic molecules in seven solvents to experiment. The chiral molecules chosen are fenchone (**1**), camphor (**2**), α-pinene (**3**), β-pinene (**4**), camphorquinone (**5**), verbenone (**6**) and methyloxirane (**7**):

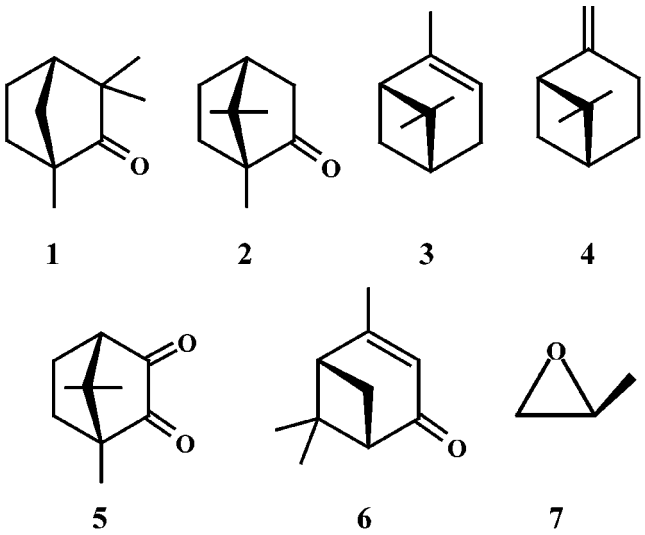

* To whom correspondence should be addressed.
† bene@dcci.unipi.it.
‡ cheese@gaussian.com.
§ pstephen@usc.edu or stephens_philip@hotmail.com.

10.1021/jp020124t CCC: $22.00
Published on Web 05/30/2002

The solvents after are C_6H_{12}, CCl_4, C_6H_6, $CHCl_3$, $(CH_3)_2CO$, CH_3OH, and CH_3CN, a diverse set. For **1**−**6**, new experimental measurements of $[\alpha]_D$ have been carried out. In the case of **7**, $[\alpha]_D$ values are taken from the literature.[2]

According to the canonical treatment of the theory of optical rotatory power,[6] the optical rotation at a frequency ν of an isotropic dilute solution of a chiral molecule is given by

$$\phi(\nu) = \frac{16\pi^3 N\nu^2}{c^2}\gamma_{LF}(\nu)\beta(\nu) \tag{1}$$

where $\phi(\nu)$ is the rotation in radians per centimeter. In eq 1, $\beta(\nu)$ is given by

$$\beta(\nu) = \frac{1}{3}\,\mathrm{Tr}[\beta_{\alpha\beta}(\nu)]$$

$$\beta_{\alpha\beta}(\nu) = \frac{c}{3\pi h}\,\mathrm{Im}\left[\sum_{k\neq 0}\frac{\langle 0|(\mu^e_{el})_\alpha|k\rangle\langle k|(\mu^e_{mag})_\beta|0\rangle}{\nu_{k0}{}^2 - \nu^2}\right] \tag{2}$$

$\beta_{\alpha\beta}(\nu)$ is the frequency-dependent electric dipole−magnetic dipole polarizability of the chiral molecule. In eq 2, 0 and k label ground and excited electronic states and μ^e_{el} and μ^e_{mag} are the electronic electric and magnetic dipole moment operators. In eq 1, $\gamma_{LF}(\nu)$ is the "local field correction factor" (i.e., the ratio of the microscopic electric field acting on the chiral molecule to the macroscopic electric field of the light wave) of Lorentz,[7] given by

$$\gamma_{LF}(\nu) = \frac{\epsilon_s(\nu) + 2}{3} = \frac{n_s(\nu)^2 + 2}{3} \tag{3}$$

where $\epsilon_s(\nu)$ and $n_s(\nu)$ are the dielectric constant and refractive index of the solvent, respectively. In eq 1, both $\gamma_{LF}(\nu)$ and $\beta(\nu)$ are solvent-dependent.

A variety of ab initio methods have recently been applied to the calculation of optical rotation.[3,8] In all calculations to date, solvent effects on β have been ignored. The local field correction has either been ignored ($\gamma_{LF} = 1$) or included using eq 3. None of these calculations satisfactorily take account of solvent effects. Calculations ignoring solvent effects on β and with $\gamma_{LF} = 1$ predict solvent-independent optical rotations. Optical rotations calculated ignoring solvent effects on β and using eq 3 for γ_{LF}, while solvent-dependent via the solvent dependence of ϵ_s and $n_s(\nu)$, are equally unsatisfactory since the Lorentz treatment of the local field correction has been discredited for many years. As further evidence of the inadequacy of this approach to the inclusion of solvent effects, we note that in recent studies of the sodium D line specific rotations, $[\alpha]_D$, of a large set of rigid, chiral organic molecules, it was found that the mean absolute deviation of $[\alpha]_D$ values predicted using DFT, a state-of-the-art functional (B3LYP), and a large basis set including diffuse functions (aug-cc-pVDZ), from experimental values was substantially smaller when the local field correction was ignored than when eq 3 was used.[3]

In formulating a theory of solvent effects on optical rotations, there are two choices to be made: (1) the quantum-mechanical methodology and (2) the solvent model. To date, the most accurate quantum-mechanical methodology already implemented is DFT,[3] and DFT is consequently used in this work. With respect to the solvent, one must choose between continuum and atomistic solvent models. The former are computationally more tractable. In this work, we use the polarizable continuum model (PCM), a continuum solvent model already well-developed and widely used in treating solvent effects on molecular properties.[9]

Theory

Given material equations of the form

$$\vec{D} = \epsilon\vec{E} - g\dot{\vec{H}}$$
$$\vec{B} = \vec{H} + g\dot{\vec{E}} \tag{4}$$

Maxwell's equations lead to optical rotation at frequency ν in radians per centimeter given by[6]

$$\phi(\nu) = \frac{4\pi^2\nu^2}{c}g(\nu) \tag{5}$$

In eq 4, ϵ is the dielectric constant; the magnetic permeability has been approximated as unity. $\vec{D}$ and $\vec{B}$ are related to the electric and magnetic polarizations per unit volume, $\vec{P}$ and $\vec{I}$, via

$$\vec{D} = \vec{E} + 4\pi\vec{P}$$
$$\vec{B} = \vec{H} + 4\pi\vec{I} \tag{6}$$

where, in a solution,

$$\vec{P} = N_m\vec{p}_m + N_s\vec{p}_s$$
$$\vec{I} = N_m\vec{m}_m + N_s\vec{m}_s \tag{7}$$

In eq 7, N_m and N_s are the numbers of solute and solvent molecules/cm^3, respectively. $\vec{p}_m$ and $\vec{p}_s$ are the electric dipole moments of solute and solvent molecules induced by the electromagnetic field. $\vec{m}_m$ and $\vec{m}_s$ are the corresponding induced magnetic dipole moments.

In the canonical theory,[6] the induced molecular moments are expanded in terms of the microscopic (effective) electromagnetic fields, $\vec{e}$ and $\vec{h}$:

$$\vec{p}_i = \alpha_i\vec{e} - \left(\frac{\beta_i}{c}\right)\dot{\vec{h}}$$
$$\vec{m}_i = \left(\frac{\beta_i}{c}\right)\dot{\vec{e}} \qquad (i = \mathrm{m, s}) \tag{8}$$

where α_i and β_i are the electric dipole polarizability and electric dipole−magnetic dipole polarizability, respectively. The microscopic and macroscopic electric fields are then connected using the Lorentz approximation:[6,7]

$$\vec{e} = \vec{E} + \frac{4}{3}\pi\vec{P} \tag{9}$$

Microscopic and macroscopic magnetic fields are taken to be equal. Assuming a chiral solute and an achiral solvent, so that $\beta_m \neq 0$ and $\beta_s = 0$, and a dilute solution, so that the solution dielectric constant is equal to that of the pure solvent, g is related to β_m via

$$g(\nu) = \frac{4\pi N_m}{c}\left(\frac{\epsilon_s(\nu) + 2}{3}\right)\beta_m(\nu) \tag{10}$$

whence follows eq 1 for $\phi(\nu)$ with γ_{LF} given by eq 3. We note that γ_{LF} is the result of two effects, which, following Onsager's notation, can be termed the "reaction-field" and the "cavity-field" effects, respectively. While the cavity-field effect depends only on the external macroscopic field, the reaction-field effect

is related to the solute dipole moment induced by the external field in the presence of the solvent.

In order to incorporate all contributions of the solvent on the optical rotation of a solute in an integrated and self-consistent manner, we here modify the canonical theory as follows. As in our previous treatment of the electric response properties of molecular solutes to external static or oscillating electric fields,[9c,g] we introduce the concept of "effective polarizabilities", specifically the effective electric polarizability, $\tilde{\alpha}$, and the effective electric dipole−magnetic dipole polarizability, $\tilde{\beta}$. Through such properties, we can directly represent the solvent-modified response of the solute to the macroscopic electromagnetic fields without the need to introduce a correction factor such as γ_{LF} (eq 3) but at the same time including the complete solvent effect. By introducing the effective polarizabilities, the induced molecular moments can be expanded directly in terms of the macroscopic Maxwell fields $\vec{E}$ and $\vec{H}$:

$$\vec{p}_i = \tilde{\alpha}_i \vec{E} - \left(\frac{\tilde{\beta}_i}{c}\right)\dot{\vec{H}}$$

$$\vec{m}_i = \left(\frac{\tilde{\beta}_i}{c}\right)\dot{\vec{E}} \qquad (i = \mathrm{m}, \mathrm{s}) \tag{11}$$

Then

$$g = \frac{4\pi N_m}{c}\tilde{\beta}_m \tag{12}$$

and

$$\phi(\nu) = \frac{16\pi^3 N_m \nu^2}{c^2}\tilde{\beta}_m \tag{13}$$

The advantage of this modification is that it allows solvent effects to be introduced in a more general way. In the following exposition, we shall show how the effective polarizability $\tilde{\beta}_m$ is calculated using the DFT/PCM methodology.

The IEF-PCM. In the PCM, originally developed in 1981[5] and reformulated in the so-called IEF version in 1997,[4] a solute molecule, treated quantum mechanically, is placed within a volume, the "solute cavity". The shape and dimensions of the cavity are determined by the molecular structure; in practice, the cavity is the envelope of spheres placed on the nuclei of the solute molecule. The cavity is surrounded by a continuum dielectric. The solute molecule polarizes the dielectric; the dielectric polarization, in turn, generates an electrostatic field at the solute molecule, modifying its electron density, ρ. The solute molecule−solvent interaction, V_{MS}, is expressed in terms of the interaction of the electrostatic potential of the solute molecule with an apparent charge density, $\sigma(s)$, on the surface of the cavity representing the polarization of the dielectric:

$$V_{MS} = \int_\Sigma V(s)[\sigma^N(s) + \sigma^e(\rho;s)]\, ds \tag{14}$$

$V(s)$ is the electrostatic potential of the solute molecule calculated on the cavity surface, Σ. The surface charge density, $\sigma(s)$, is partitioned into contributions from the nuclei and electrons of the solute, $\sigma^N(s)$ and $\sigma^e(\rho;s)$, respectively. The dependence of σ^e on the solute molecule electron density ρ is indicated explicitly. The surface charge density, $\sigma(s)$, is a function of the solute molecule charge density, ρ, the cavity, and the solvent dielectric constant, ϵ_s.

In the presence of the macroscopic Maxwell electric field of frequency $\omega = 2\pi\nu$,

$$\vec{E} = \vec{E}^\omega(e^{i\omega t} + e^{-i\omega t})/2 \tag{15}$$

the complete Hamiltonian of the solute molecule can be written

$$H = H^\circ + V_{MS} + V'(t) \tag{16}$$

where H° is the Hamiltonian in vacuo and the time-dependent perturbation, $V'(t)$, is given by

$$V'(t) = -{}^1/_2(\mu^e_{el})_\alpha E^\omega_\alpha(e^{i\omega t} + e^{-i\omega t}) - {}^1/_2\int_\Sigma V(s)\frac{\partial\sigma^{ex}_\omega(s)}{\partial E^\omega_\alpha}E^\omega_\alpha(e^{i\omega t} + e^{-i\omega t})\, ds \tag{17}$$

(repeated indices are summed over). In eq 17, a new apparent surface charge density, $\sigma^{ex}_\omega(s)$, has been introduced, representing the response of the solvent to the external field after creation of the solute cavity in the solvent. This term describes the cavity-field effect that we have previously introduced as one of the two terms included in the Lorentz "local field correction". This surface charge density must be added to those representing the solute−solvent interaction, σ^N and σ^e, to fully describe the response of the solvent to the combined action of the field of the solute molecule and the external field. σ^{ex} is a function of the cavity and the solvent dielectric constant.[9c,g] In computing V_{MS} and $V'(t)$, surface charge densities are discretized by partitioning the cavity surface into K small portions (tesserae) of area a_k. To the kth tessera, we associate a point charge $q_k = a_k\sigma(s_k)$, which is placed at the geometrical center, s_k, of the tessera. The charges q_k are obtained by solving a matrix equation of the type:

$$\mathbf{q}^x = -\mathbf{Q}(\epsilon)\mathbf{V}^x \qquad (x = e, N) \tag{18}$$

where $\mathbf{Q}$ is a square matrix that depends on the solvent dielectric constant ϵ and the geometrical parameters defining the molecular cavity, and $\mathbf{V}$ is a vector collecting (electronic or nuclear) potential values computed on tesserae. Within this framework, the surface integrals in eqs 14 and 17 then reduce to summations over K tesserae.

Equation 17 expresses the time-dependent perturbation on the solute molecule in terms of the external Maxwell electric field, and it allows us to directly calculate the linear response of the molecule to this field, that is, the effective polarizabilities of the molecule. In the following section, we shall show how to calculate the effective polarizability $\tilde{\beta}_m$ required to predict the optical rotation via eq 13.

DFT/PCM Calculation of $\tilde{\beta}(\nu)$. Before presenting the expressions used to calculate $\tilde{\beta}_m$ of solvated molecules within the DFT/PCM framework, we summarize the basic theory for isolated molecules. As shown in the Introduction, the frequency-dependent electric dipole−magnetic dipole polarizability tensor, $\beta_{\alpha\beta}$, can be expressed in terms of a sum of products of electric and magnetic transition dipoles between ground and excited states (see eq 2). Such sum-over-states has been reexpressed within the framework of time-dependent linear-response theory for self-consistent field (SCF), either Hartree−Fock (HF) or DFT, multiconfigurational SCF, and coupled-cluster wave functions.[10]

For SCF wave functions, in the limit of a static field, the explicit evaluation of the sum-over-states can be avoided by rewriting $\beta_{\alpha\beta}$ in terms of electric and magnetic field derivatives of the ground-state electronic wave function.[11] This expression can be generalized to the frequency-dependent case using linear response theory, when

$$\beta_{\alpha\beta}(\omega) = \frac{hc}{3\pi}\,\mathrm{Im}\left\langle \frac{\partial\Psi(\omega)}{\partial E_\alpha}\middle|\frac{\partial\Psi(\omega)}{\partial H_\beta}\right\rangle = \frac{hc}{3\pi}\,\mathrm{Im}\left[\sum_{\mu\nu} D_{\mu\nu}^{E_\alpha}\langle\chi_\mu|\chi_\nu^{H_\beta}\rangle + \sum_{\mu\nu} D_{\mu\nu}^{E_\alpha H_\beta}\langle\chi_\mu|\chi_\nu\rangle\right] \quad (19)$$

where E_α and H_β are electric and magnetic field, respectively, and superscripts denote differentation with respect to the variable indicated. The atomic basis functions, χ_μ, are magnetic-field-dependent to ensure the gauge independence of β, and $\mathbf{D}^x$ are the following half-derivative density matrices:

$$D_{\mu\nu}^{E_\alpha} = \sum_i c_{\mu i}^{E_\alpha(\mathrm{real})} c_{\nu i}$$

$$D_{\mu\nu}^{E_\alpha H_\beta} = \sum_i c_{\mu i}^{E_\alpha(\mathrm{real})}\, c_{\nu i}^{H_\beta(\mathrm{imag})} + \sum_i c_{\mu i}^{E_\alpha(\mathrm{imag})}\, c_{\nu i}^{H_\beta(\mathrm{real})} \quad (20)$$

where $c_{\mu i}$ are the time-dependent molecular orbital coefficients and single superscripts denote differentiation with respect to the variable indicated.

The gauge-independent atomic orbital (GIAO) magnetic-field-dependent basis functions, χ_μ, used in eq 19 are given by[12]

$$\chi_\mu(\mathbf{H}) = \exp\left[-\frac{i}{2c}(\mathbf{H}\times\mathbf{R}_\mu)\cdot\mathbf{r}\right]\chi_\mu(0) \quad (21)$$

where $\mathbf{R}_\mu$ is the position vector of basis function χ_μ and $\chi_\mu(0)$ denotes the usual field-independent basis function.

The change in the molecular orbital coefficients with respect to oscillating applied electric or magnetic field perturbations required to compute the half-derivative matrices of eq 20 is determined from the time-dependent equation

$$\mathbf{FC} - i\frac{\partial}{\partial t}(\mathbf{SC}) = \mathbf{SC}\epsilon \quad (22)$$

with the orthonormality condition

$$\frac{\partial}{\partial t}(\mathbf{C}^+\mathbf{SC}) = 0 \quad (23)$$

where $\mathbf{C}$, $\mathbf{S}$, and ϵ are orbital coefficient, overlap, and orbital energy matrices. The Fock matrix, $\mathbf{F}$, is

$$\mathbf{F} = \mathbf{h} + \mathbf{G}(\mathbf{P}); \quad \mathbf{G}(\mathbf{P})_{\mu\nu} = \langle\mu\lambda||\nu\sigma\rangle\mathbf{P}_{\lambda\sigma} + \chi_{\mathrm{xc}}(\mathbf{P})_{\mu\nu}$$

$$\chi_{\mathrm{xc}} = \frac{\partial E_{\mathrm{xc}}}{\partial\zeta}\frac{\partial\zeta}{\partial\mathbf{P}}; \quad E_{\mathrm{xc}} = \int f(\zeta)\,\mathrm{d}\mathbf{r} \quad (24)$$

where $\mathbf{h}$ is the one-electron Hamiltonian, $\mathbf{P}$ is the density matrix, and the (antisymmetrized) two-electron integrals include a coefficient for Hartree−Fock exchange, which is one for Hartree−Fock, zero for pure DFT, and nonzero for hybrid methods. χ_{xc} is the exchange−correlation contribution to the Fock matrix. E_{xc} is the exchange−correlation energy, which is a functional of the spin densities and density-gradient invariants (collection denoted by ζ) represented by f, a general first-order real exchange−correlation functional, which is frequency-independent and does not include an explicit magnetic-field-dependent term.[13]

The one-electron Hamiltonian for a system subjected to an oscillating (electric or magnetic) field can be expressed as[14]

$$\mathbf{h} = \mathbf{h}_0 + \mathbf{h}'(\omega); \quad \mathbf{h}'(\omega) = \frac{1}{2}(\mathbf{L}\,\mathrm{e}^{-i\omega t} + \mathbf{L}^+\,\mathrm{e}^{i\omega t}) \quad (25)$$

where $\mathbf{h}_0$ describes the unperturbed system in a stationary state and $\mathbf{h}'(\omega)$ is the response to a single oscillatory perturbation described by $\mathbf{L}$. The time-dependent stationary-value condition (eq 22) can be rewritten in terms of the density matrix in the molecular orbital basis as

$$\mathbf{FPS} - \mathbf{SPF} = i\frac{\partial}{\partial t}\mathbf{P} \quad (26)$$

Expressing the relaxed density matrix as

$$\mathbf{P} = \mathbf{P}_0 + \frac{1}{2}(\mathbf{U}\,\mathrm{e}^{-i\omega t} + \mathbf{U}^+\,\mathrm{e}^{i\omega t}) \quad (27)$$

and expanding to first order in $\mathbf{U}$ yields the two coupled equations

$$(\epsilon_i - \epsilon_a)\mathbf{X}_{ai} - \mathbf{R}_{ai}^* - \mathbf{G}'(\mathbf{X}^*,\mathbf{Y})_{ia} = -\omega\mathbf{X}_{ai}$$
$$(\epsilon_i - \epsilon_a)\mathbf{Y}_{ai} - \mathbf{R}_{ia} - \mathbf{G}'(\mathbf{Y}^*,\mathbf{X})_{ia} = \omega\mathbf{X}_{ai} \quad (28)$$

after collecting terms in $\mathrm{e}^{\pm i\omega t}$, projecting out the occupied-virtual blocks, substituting $\mathbf{X}_{ia} = \mathbf{U}_{ia}$ and $\mathbf{Y}_{ia} = \mathbf{U}_{ai}^*$ and introducing

$$\mathbf{G}'(\mathbf{M}^*,\mathbf{N})_{ia} = \langle ib||aj\rangle\mathbf{M}_{bj} + \langle ij||ab\rangle\mathbf{N}_{bj} + \chi'_{\mathrm{xc}}(\mathbf{M}+\mathbf{N})_{bj}$$
$$\chi'_{\mathrm{xc}} = \frac{\partial\chi_{\mathrm{xc}}}{\partial\zeta}\frac{\partial\zeta}{\partial\mathbf{P}} \quad (29)$$

where i and j refer to occupied orbitals and a and b refer to virtual orbitals. Expressing eq 28 in terms of the orbital rotation Hessian, $\mathbf{A}+\mathbf{B}$, and the magnetic Hessian, $\mathbf{A}-\mathbf{B}$, where

$$(\mathbf{A}+\mathbf{B})_{ia,jb} = \langle ib||aj\rangle + \langle ij||ab\rangle + \chi'_{ia,jb} + (\epsilon_a - \epsilon_i)\delta_{ai,bj}$$
$$(\mathbf{A}-\mathbf{B})_{ia,jb} = \langle ij||ab\rangle + \langle ib||aj\rangle + (\epsilon_a - \epsilon_i)\delta_{ai,bj} \quad (30)$$

yields the following coupled system of equations:[15]

$$\begin{pmatrix}\mathbf{A}-\omega\mathbf{I} & \mathbf{B}\\ \mathbf{B}^+ & \mathbf{A}+\omega\mathbf{I}\end{pmatrix}\begin{pmatrix}\mathbf{X}\\ \mathbf{Y}\end{pmatrix} = \begin{pmatrix}\mathbf{R}_x\\ \mathbf{R}_y\end{pmatrix} \quad (31)$$

For real perturbations (electric fields), $\mathbf{R}_x = \mathbf{R}_y$, and for pure imaginary perturbations (magnetic fields), $\mathbf{R}_x = -\mathbf{R}_y$, where the occupied-virtual block of the $\mathbf{R}$ matrix is

$$\mathbf{R}_{\mathrm{ov}} = \mathbf{h}_{\mathrm{ov}}^{\mathrm{pert}} + \mathbf{G}_{\mathrm{ov}}^{\mathrm{pert}}(\mathbf{P})_{\mathrm{ov}} - \mathbf{FS}_{\mathrm{ov}}^{\mathrm{pert}} + \mathbf{G}(\mathbf{S}_{\mathrm{oo}}^{\mathrm{pert}})_{\mathrm{ov}} \quad (32)$$

and the superscript pert refers to an electric or magnetic field perturbation, $-(\mu_{\mathrm{el}}^{\mathrm{e}})_\alpha E_\alpha$ or $-(\mu_{\mathrm{mag}}^{\mathrm{e}})_\beta H_\beta$, respectively. The above coupled perturbed (CP) equations (eq 31) are solved for $\mathbf{X}$ and $\mathbf{Y}$ together forming the products $(\mathbf{A}+\mathbf{B})(\mathbf{X}+\mathbf{Y})$ and $(\mathbf{A}-\mathbf{B})(\mathbf{X}-\mathbf{Y})$ (where $(\mathbf{X}+\mathbf{Y})$ is symmetric, $(\mathbf{X}-\mathbf{Y})$ is antisymmetric, and $(\mathbf{A}+\mathbf{B})(\mathbf{X}-\mathbf{Y}) = (\mathbf{A}-\mathbf{B})(\mathbf{X}+\mathbf{Y}) = 0$) and using a separate expansion space for each perturbation at each frequency.[16] The derivatives of the molecular orbital expansion coefficients have real and imaginary parts for both electric and magnetic perturbations

$$c_{\mu p}^{\mathrm{pert(real)}}(\omega) = \sum_q (\mathbf{X}_{qp} + \mathbf{Y}_{pq})c_{\mu q}$$
$$c_{\mu p}^{\mathrm{pert(imag)}}(\omega) = \sum_q (\mathbf{X}_{qp} - \mathbf{Y}_{pq})c_{\mu q} \quad (33)$$

which are used to construct the half-derivative density matrices in eq 20.

In the presence of a continuum dielectric using the IEF-PCM, the frequency-dependent perturbation defined in eq 25 can be rewritten as (see eq 17)

$$\mathbf{h}' = \frac{1}{2}\sum_{\alpha}\mathbf{m}_{\alpha}^{\mathrm{elec}}E_{\alpha}(\mathrm{e}^{-i\omega t} + \mathrm{e}^{i\omega t}) + \frac{1}{2}\sum_{\alpha}\sum_{s}\mathbf{V}(s)\frac{\partial \mathbf{q}^{\mathrm{ex}}(s)}{\partial E_{\alpha}}E_{\alpha}(\mathrm{e}^{-i\omega t} + \mathrm{e}^{i\omega t}) \quad (34)$$

where we have assumed that the oscillating field is the Maxwell electric field with strength **E** and $\mathbf{m}^{\mathrm{elec}}$ is the electric dipole integrals matrix (namely, $\mathbf{L} = \mathbf{m}\cdot\mathbf{E}$). In eq 34, **V** is the vector collecting the potential integrals computed on the cavity tesserae and $\mathbf{q}^{\mathrm{ex}}$ is the vector of the apparent charge induced on the cavity by the external oscillating field. Equation 34 when summed to the Hamiltonian modified by the solvent terms described by $\mathbf{q}^{N}$ and $\mathbf{q}^{e}$, allows one to take into account the complete reaction of the solvent to the combined action of the internal (due to the solute) and the external fields.

Approximate solutions of the time-dependent equations resulting from the effective Hamiltonian can be obtained using the same procedures formulated for isolated molecules. Equations 22 and 26 are still valid but the Fock operator **F** has to be modified to include solvent terms:

$$\mathbf{F}' = \mathbf{F}_{\mathrm{vac}} + [\mathbf{j} + \mathbf{X}(\mathbf{P})] + \frac{1}{2}\sum_{\alpha}\tilde{\mathbf{m}}_{\alpha}(\omega)E_{\alpha}(\mathrm{e}^{-i\omega t} + \mathrm{e}^{i\omega t}) \quad (35)$$

where $\mathbf{F}_{\mathrm{vac}}$ is the Fock matrix for the isolated molecule in the presence of the oscillating field. The first two solvent-induced terms, **j** and **X**(**P**), reflect the constant and the density-matrix-dependent components of the reaction potential V_{MS} defined in eq 14 and are defined as sums over all cavity tesserae of products of electronic potential integrals and solvent apparent charges. In the last term, $\tilde{\mathbf{m}}$ is the matrix related to the apparent charges, $\mathbf{q}^{\mathrm{ex}}(\omega;s)$, induced by the external oscillating field, namely,[9c]

$$\tilde{\mathbf{m}}_{\alpha}(\omega) = \sum_{s}\mathbf{V}(s)\frac{\partial \mathbf{q}^{\mathrm{ex}}(\omega;s)}{\partial E_{\alpha}} \quad (36)$$

where we have made explicit the dependence of the apparent charges and of the resulting $\tilde{\mathbf{m}}$ matrix on the frequency ω of the applied field; such dependence is obtained by using a frequency-dependent dielectric constant, $\epsilon(\omega)$, to compute the apparent charges.

The first-order variations of the molecular orbital coefficients are still obtained by solving the system of eq 31 in which now both orbitals and orbital energies are modified with respect to the isolated molecule and the orbital rotation Hessian becomes[17]

$$(\mathbf{A} + \mathbf{B})_{ia,jb} = \langle ib||aj\rangle + \langle ij||ab\rangle + \chi'_{ia,jb} + (\epsilon_a - \epsilon_i)\delta_{ai,bj} + 2\mathbf{B}_{ai,bj} \quad (37)$$

and the $\mathbf{h}_{\mathrm{ov}}^{\mathrm{pert}}$ to be used in the **R** matrix reduces to

$$\mathbf{h}_{\mathrm{ov}}^{\mathrm{pert}} = \mathbf{m}_{\mathrm{ov}}^{\mathrm{elec}} + \tilde{\mathbf{m}}_{\mathrm{ov}} \quad (38)$$

In eq 37, the solvent-induced integrals are

$$\mathbf{B}_{ai,bj} = \sum_{s}\mathbf{V}_{ai}(s)\mathbf{q}_{bj}(s) \quad (39)$$

where we have introduced a new charge matrix **q** defined in the molecular orbital basis as

$$\mathbf{q}_{bj} = -\mathbf{Q}(\epsilon)\mathbf{V}_{bj} \quad (40)$$

where **Q** is the dielectric matrix defining the solvent apparent charge. This matrix depends on the cavity geometry and on the solvent dielectric constant ϵ, and thus, in the present case in which an oscillating field is applied, it will depend on the frequency-dependent $\epsilon(\omega)$. The inclusion of the additional solvent terms in the CP equations will lead to different values of the derivatives of the molecular orbital expansion coefficients for an electric perturbation, $c_{\mu i}^{E_{\alpha}}$, and thus to solvent-modified half-derivative density matrices (eq 20).

The mixed nature of the electric dipole−magnetic dipole polarizability $\tilde{\beta}$ requires an additional CP procedure containing a magnetic perturbation. Due to the imaginary nature of this perturbation, solvent-induced terms do not appear in the corresponding $\mathbf{h}_{\mathrm{ov}}^{\mathrm{pert}}$ matrix and only contribute to the first-order expansion term of the Fock operator through a term induced by the dependence of the atomic orbital basis set on the magnetic field;[9a,9d] as a consequence, the derivatives of the molecular orbitals with respect to the magnetic field, which are used to construct the half-derivative density matrices in eq 20, will also be modified by the solvent.

As a final note, it is important to remark that both solvent contributions to the electric perturbation, namely, **B** and $\tilde{\mathbf{m}}$ matrices of eqs 37 and 38, are obtained in terms of solvent charges, which are calculated using the value of the dielectric constant at the frequency of the external field. In the present case, this is the sodium D line frequency and thus the value for $\epsilon(\omega)$ coincides with the so-called optical dielectric constant, ϵ_{opt}, defined as the square of the refractive index. For polar solvents, ϵ_{opt} is much smaller than the static ϵ_0 analogue; the solvent response determined by ϵ_{opt} is thus much smaller than that in the presence of a static field. This situation is usually defined as the "nonequilibrium" solute−solvent regime, while that corresponding to a full solvent response is termed the "equilibrium" regime.[18]

Experimental and Computational Methods

Specific rotations, $[\alpha]_{\mathrm{D}}$, of **1**−**6** were measured at 25 °C using a Perkin-Elmer model 241 polarimeter. Single enantiomers of **1**−**6**, purchased from Aldrich, were used: **1**, (1R)-(−)-**1**, $[\alpha]_{\mathrm{D}} = -50.5°$ (neat); **2**, (1R)-(+)-**2**, $[\alpha]_{\mathrm{D}} = 44.1°$ ($c = 10$, C_2H_5OH); **3**, (1R)-(+)-**3**, $[\alpha]_{\mathrm{D}} = 50.7°$ (neat); **4**, (1S)-(−)-**4**, $[\alpha]_{\mathrm{D}} = -22°$ (neat); **5**, (1R)-(−)-**5**, $[\alpha]_{\mathrm{D}} = -101°$ ($c = 2$, $C_6H_5CH_3$); **6**, (1S)-(−)-**6**, $[\alpha]_{\mathrm{D}} = -142°$ (neat). Solvents were as follows: C_6H_{12}, spectro grade, Aldrich; CCl_4, anhydrous, Aldrich; C_6H_6, spectro grade, Aldrich; $CHCl_3$, spectro grade, Aldrich; $(CH_3)_2CO$, spectro grade, Aldrich; CH_3OH, spectro grade, Aldrich; CH_3CN, spectro grade, Aldrich. Solution concentrations were 0.1 M. All samples were close to 100% ee. Measured $[\alpha]_{\mathrm{D}}$ values were not corrected to 100% ee.

DFT calculations of $[\alpha]_{\mathrm{D}}$ were carried out using the B3LYP functional and the aug-cc-pVDZ basis set[3] at B3LYP/6-31G* equilibrium geometries. IEF-PCM calculations were carried out using molecular cavities obtained from intersecting spheres centered on heavy atoms: the radii used for the carbon-centered spheres were 2.04 Å, 2.28 Å (if the carbon was bonded to one or two hydrogens), and 2.8 Å (if the carbon was bonded to three hydrogens), and the radius used for oxygen was 1.5 Å. The solvents were described in terms of their static and optical dielectric constants: 2.028 ($\epsilon(0) = \epsilon_{\mathrm{opt}}$) for C_6H_{12}, 2.228 and 2.129 for CCl_4, 2.247 and 2.244 for C_6H_6, 4.90 and 2.085 for

TABLE 1: Calculated and Experimental $[\alpha]_D$ Values for 1−7[a]

	gas	C_6H_{12}	CCl_4	C_6H_6	$CHCl_3$	$(CH_3)_2CO$	CH_3OH	CH_3CN
				1S-(+)-Fenchone, **1**				
dyn	67.4							
stat	51.8							
dyn/neq		85.3	86.4	85.8	93.2	97.7	97.7	98.1
dyn/g_vac		78.3	79.2	79.5	83.3	86.2	86.3	86.6
dyn/eq		85.3	86.6	85.8	96.3	103.9	104.7	104.8
stat/eq		64.4	65.2	64.5	71.6	76.6	77.1	77.3
Lorentz		90.6	92.8	95.6	91.9	86.4	84.6	85.5
expt		45.6	55.2	60.1	62.1	51.3	60.9	55.7
				(1R,4R)-(+)-Camphor, **2**				
dyn	60.7							
stat	36.0							
dyn/neq		64.0	63.8	64.4	58.9	53.5	52.6	52.9
dyn/neq/lf		70.3	70.2	71.1	64.2	57.6	56.4	56.7
dyn/eq		63.9	64.3	64.4	67.4	69.7	70.0	70.1
stat/eq		38.1	38.4	38.4	40.3	41.6	41.9	41.9
Lorentz		81.6	83.6	86.1	82.8	77.8	76.2	77.0
expt		57.1	43.3	38.3	39.3	47.3	36.8	42.6
				1R-(+)-α-Pinene, **3**				
dyn	41.9							
stat	41.3							
dyn/neq		44.7	44.6	44.2	46.6	48.4	49.1	48.6
dyn/eq		45.0	44.5	44.5	37.9	23.9	21.9	20.9
stat/eq		44.6	44.4	44.3	39.3	28.1	26.5	25.7
Lorentz		56.3	57.7	59.4	57.2	53.7	52.6	53.2
expt		49.1	54.4	50.2	58.1	54.2	56.3	59.9
				1R-(+)-*β*-Pinene, **4**				
dyn	26.4							
stat	8.1							
dyn/neq		26.2	30.2	26.6	26.5	26.1	26.0	26.1
dyn/eq		26.2	30.3	26.6	29.3	32.3	32.6	32.6
stat/eq		5.9	9.0	6.0	6.7	7.7	7.7	7.7
Lorentz		35.5	36.4	37.4	36.0	33.8	33.1	33.5
expt		18.4	25.1	29.9	18.1	15.2	15.9	12.9
				1S-(+)-Camphorquinone, **5**				
dyn	142.4							
stat	48.3							
dyn/neq		146.4	147.6	146.7	157.7	165.7	166.9	166.5
dyn/eq		146.5	146.6	146.6	138.4	124.3	122.3	121.4
stat/eq		48.4	48.2	48.2	45.6	42.5	42.1	41.9
Lorentz		191.4	196.1	201.9	194.2	182.6	178.7	180.7
expt		94.4	91.9	103.3	97.6	117.1		111.6
				1R-(+)-Verbenone, **6**				
dyn	258.7							
stat	164.1							
dyn/neq		286.8	288.5	290.6	286.6	281.3	278.8	280.3
dyn/g_vac		282.1	282.9	284.6	277.8	270.5	268.4	269.4
dyn/eq		286.7	290.1	290.6	307.2	315.7	315.5	316.1
stat/eq		182.0	183.8	184.3	192.5	194.4	193.5	193.9
Lorentz		347.7	356.2	366.8	352.9	331.7	324.7	328.3
expt		175.3	175.2	171.6	183.5	179.8	169.6	171.7
				2R-(+)-Methyloxirane, **7**				
dyn	17.5							
stat	22.5							
dyn/neq		14.7	14.2	14.1	11.6	9.2	8.9	9.4
dyn/eq		14.7	14.2	14.1	10.6	7.0	6.5	7.2
stat/eq		19.5	19.0	18.9	15.3	11.7	11.2	11.8
Lorentz		23.5	24.1	24.8	23.9	22.4	21.9	22.2
expt		11.9	18.7	30.6	8.5	8.2	7.2	6.0

[a] All $[\alpha]_D$ values are in degrees $[\mathrm{dm\ g/cm^3}]^{-1}$. All calculations were carried out using the B3LYP functional and the aug-cc-pVDZ basis set. See text for details on the different solvation models used to obtain the various sets of results.

$CHCl_3$, 20.7 and 1.841 for $(CH_3)_2CO$, 32.63 and 1.758 for CH_3OH, and 36.64 and 1.806 for CH_3CN. All calculations were carried out using the Gaussian program.[19]

Results

Experimental $[\alpha]_D$ values of **1**−**7** in the seven chosen solvents are given in Table 1 and plotted in Figure 1. The most striking feature of these results is that the variation of $[\alpha]_D$ with solvent is highly molecule-dependent. No two molecules exhibit the same ordering of $[\alpha]_D$ values with respect to solvent variation. This is particularly surprising in the case of very similar molecules. Thus, one might expect the $[\alpha]_D$ values of fenchone, **1**, and camphor, **2**, two very similar molecules, to exhibit similar solvent dependence. Instead, the ordering of $[\alpha]_D$ for **2**, CH_3OH

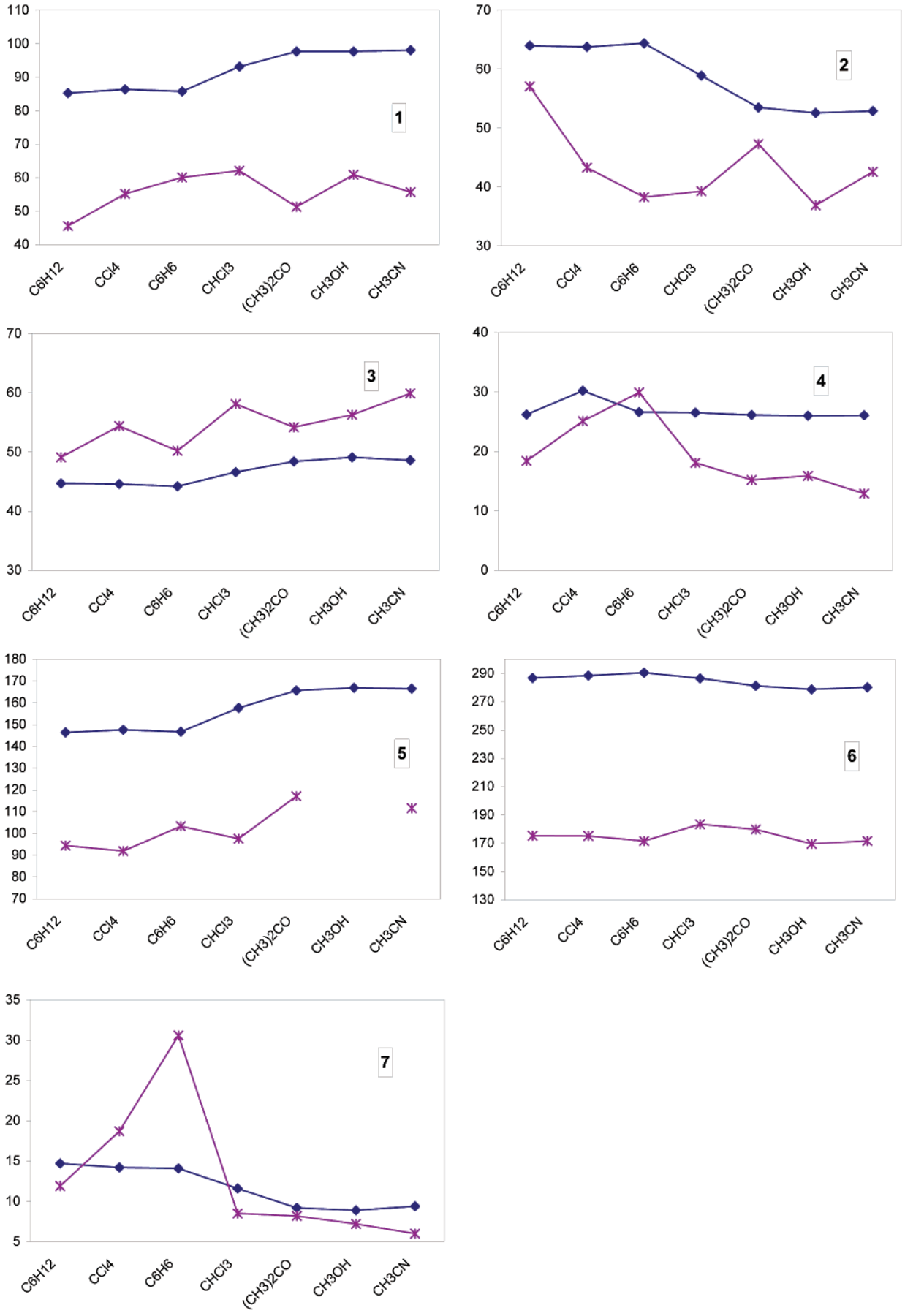

Figure 1. Calculated and experimental $[\alpha]_D$ values for **1**−**7** in the various solvents: (◆) dynamic/nonequilibrium; (*) experiment.

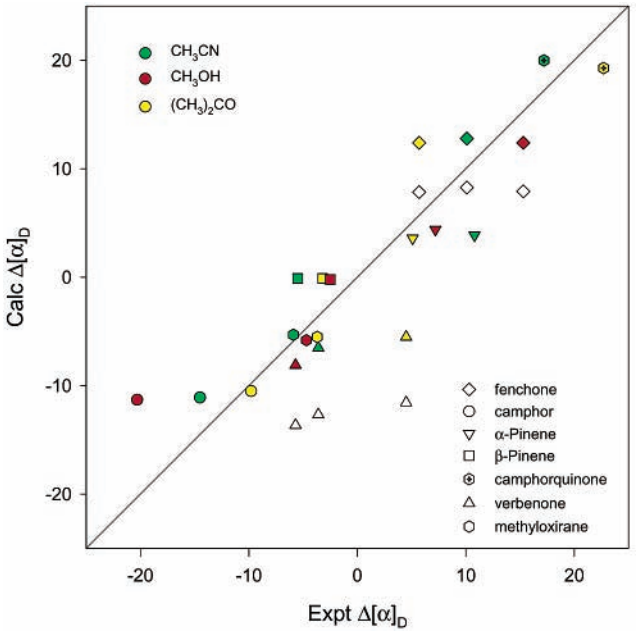

Figure 2. Comparison of calculated dynamic/nonequilibrium and experimental variations in $[\alpha]_D$ values for **1**−**7** in $(CH_3)_2CO$, CH_3OH, and CH_3CN. $\Delta[\alpha]_D$ is the difference in $[\alpha]_D$ from that in C_6H_{12}. The line is of slope +1.

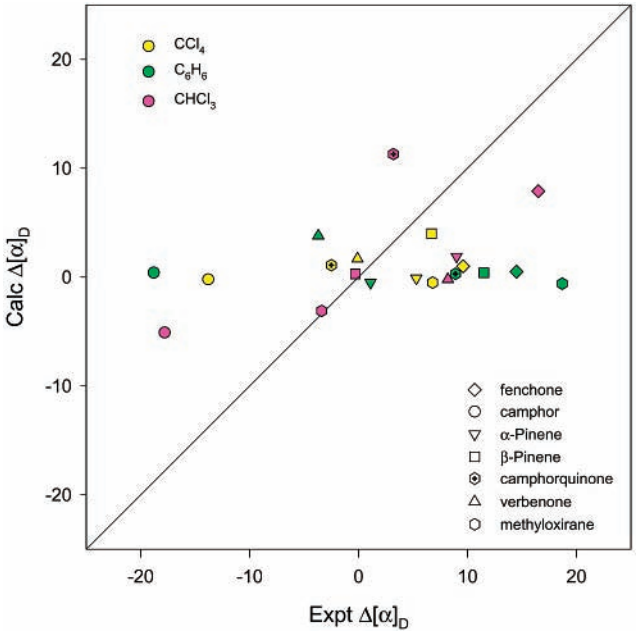

Figure 3. Comparison of calculated dynamic/nonequilibrium and experimental variations in $[\alpha]_D$ values for **1**−**7** in CCl_4, C_6H_6, and $CHCl_3$. $\Delta[\alpha]_D$ is the difference in $[\alpha]_D$ from that in C_6H_{12}. The line is of slope +1.

$< C_6H_6 < CHCl_3 < CH_3CN < CCl_4 < (CH_3)_2CO < C_6H_{12}$, is, with the exception of $CHCl_3$, exactly opposite to that for **1**, $C_6H_{12} < (CH_3)_2CO < CCl_4 < CH_3CN < C_6H_6 < CH_3OH < CHCl_3$.

$[\alpha]_D$ values calculated for **1**−**7** using the IEF-PCM are also given in Table 1 and Figure 1. DFT calculations use the B3LYP functional and the aug-cc-pVDZ basis set. The parameter $\tilde{\beta}$ is calculated at the sodium D line frequency: $\tilde{\beta}(D)$. The "nonequilibrium" solvent model is used, while the cavity-field effect (the second term in the rhs of eq 17) is not included. We refer to these calculations as "dynamic/nonequilibrium" (rows indicated as dyn/neq in Table 1).

We note, first, that for each molecule predicted $[\alpha]_D$ values are very similar for the three nonpolar, low-dielectric-constant solvents C_6H_{12}, CCl_4, and C_6H_6. Likewise, $[\alpha]_D$ values are also quite similar for the three polar, high-dielectric-constant solvents $(CH_3)_2CO$, CH_3OH, and CH_3CN. $[\alpha]_D$ for the solvent of intermediate polarity and dielectric constant, $CHCl_3$, is intermediate. Thus, calculated $[\alpha]_D$ values vary essentially monotonically with solvent dielectric constant. As observed previously for PCM calculations of other properties,[9] the variation is nonlinear and exhibits "saturation" with increasing dielectric constant. At the same time, the IEF-PCM calculations predict changes in $[\alpha]_D$ with solvent, which vary widely with molecule, both in magnitude and sign. Thus, for **1**, $[\alpha]_D$ varies from 85.3° (C_6H_{12}) to 98.1° (CH_3CN), a range of 12.8°, $[\alpha]_D$ increasing with increasing dielectric constant. For **2**, $[\alpha]_D$ varies from 52.6° (CH_3OH) to 64.0° (C_6H_{12}), a range of 11.4°, $[\alpha]_D$ decreasing with increasing dielectric constant.

Comparison of experimental and calculated variations in $[\alpha]_D$ with solvents shows reasonably good correlation between theory and experiment for the solvents C_6H_{12}, $(CH_3)_2CO$, CH_3OH, and CH_3CN but poor correlation for the solvents CCl_4, C_6H_6, and $CHCl_3$. The calculated and experimental changes in $[\alpha]_D$ from C_6H_{12} to $(CH_3)_2CO$, CH_3OH, and CH_3CN and from C_6H_{12} to CCl_4, C_6H_6, and $CHCl_3$ are compared in Figures 2 and 3, respectively. From C_6H_{12} to $(CH_3)_2CO$, CH_3OH, and CH_3CN, both calculated and experimental $[\alpha]_D$ values increase for **1**, **3**, and **5** and decrease for **2**, **4**, **6**, and **7**. Quantitative agreement is also quite good: the average of the absolute magnitudes of the differences between calculated and experimental changes in $[\alpha]_D$ from C_6H_{12} to $(CH_3)_2CO$, CH_3OH, and CH_3CN is 3°. On the other hand, for the changes from C_6H_{12} to CCl_4, C_6H_6, and $CHCl_3$, the correlation between theory and experiment is very poor. Experimental changes are on average much larger than predicted changes. The average of the absolute magnitudes of the differences between calculated and experimental changes in $[\alpha]_D$ from C_6H_{12} to CCl_4, C_6H_6, and $CHCl_3$ is 8°.

The finding that the dynamic/nonequilibrium DFT/PCM calculations for C_6H_{12}, $(CH_3)_2CO$, CH_3OH, and CH_3CN account quite well for the observed changes in $[\alpha]_D$ in these solvents suggests that the latter are primarily electrostatic in origin. Conversely, the finding that calculations for CCl_4, C_6H_6, and $CHCl_3$ account poorly for the observed changes in $[\alpha]_D$ in these solvents suggests that the changes are not primarily electrostatic in origin.

For comparison to the dynamic/nonequilibrium DFT/PCM calculations, we have also carried out calculations referred to as "static/equilibrium" calculations, in which $\tilde{\beta}$ is calculated in the static limit ($\nu = 0$) and the "equilibrium" solvent model is used. The functional and basis set are again B3LYP and aug-cc-pVDZ. The results are given in Table 1 (rows indicated as stat/eq). In molecules **1**, **4**, and **7**, the variation in $[\alpha]_D$ with solvent predicted by the static/equilibrium calculations is very similar to that predicted by the dynamic/nonequilibrium calculations. However, for the molecules **2**, **3**, **5**, and **6**, the results are quite different for the polar high-dielectric-constant solvents, and in much worse agreement with experiment. Overall, it is clear that the static/equilibrium calculations of solvent variations in $[\alpha]_D$ are much less accurate than the dynamic/nonequilibrium calculations.

In the static/equilibrium calculations, there are two major changes relative to the dynamic/nonequilibrium calculations: (1) the change from $\tilde{\beta}(D)$ to $\tilde{\beta}(0)$ and (2) the change from the nonequilibrium solvent model to the equilibrium solvent model. In order to define which of these changes is more important in

the change in predicted solvent effects on $[\alpha]_D$, we have carried out calculations in which $\tilde{\beta}$ is computed at the sodium D line frequency but the equilibrium solvent model is used. The results of these "dynamic/equilibrium" calculations are given in Table 1 (rows indicated as dyn/eq). The variations in $[\alpha]_D$ with solvent are very similar to those predicted by the static/equilibrium calculations; thus, the differences between the dynamic/nonequilibrium and static/equilibrium results originate predominantly in the difference in the solvent model.

All IEF-PCM calculations of $[\alpha]_D$ discussed above have been carried out using DFT/PCM molecular geometries calculated using B3LYP and the 6-31G* basis set. In order to examine the contribution to the variation in $[\alpha]_D$ with solvent of the solvent-induced change in molecular geometry, we have carried out dynamic/nonequilibrium calculations of $[\alpha]_D$ for two molecules, **1** and **6**, using the molecular geometries obtained in the absence of solvent: "gas phase" geometries. The results are given in Table 1 (rows indicated as dyn/g_vac). In both **1** and **6**, $[\alpha]_D$ values calculated using gas-phase geometries are intermediate between $[\alpha]_D$ values calculated in the absence of solvent and DFT/PCM values, and much closer to the latter. The differences between $[\alpha]_D$ values calculated with and without solvent perturbation of the molecular geometry increase with increasing solvent dielectric constant. The changes in $[\alpha]_D$ from C_6H_{12} to $(CH_3)_2CO$, CH_3OH, and CH_3CN are in somewhat worse agreement with experiment when solvent effects on the molecular geometry are not included. This supports the conclusions that (1) changes in solute molecular geometry due to interaction with the solvent are a significant factor in the variation in $[\alpha]_D$ and (2) changes in solute molecular geometry due to interaction with the solvent are reliably predicted by the DFT/PCM methodology.

Since experimental $[\alpha]_D$ values for gaseous **1**−**7** are not available, we are not able to compare predicted changes in $[\alpha]_D$ from the gas phase to solutions to experiment. $[\alpha]_D$ values in C_6H_{12} are uniformly closest to the gas-phase $[\alpha]_D$ values. Interestingly, there is considerable variation in the magnitude of the predicted change in $[\alpha]_D$ from the gas phase to C_6H_{12}. In **2**, **3**, **4**, **5**, and **7**, the changes are small, less than 5°. However, in **1** and **6**, the changes are much larger: 18° and 28°, respectively. We have no qualitative explanation at present for the much larger changes for **1** and **6**; in particular, we cannot explain why the change in **1** is much larger than that in the very similar molecule **2**.

For comparison to the predictions of the DFT/PCM methodology, we have also examined the results predicted using gas-phase DFT calculations for $[\alpha]_D$ together with the Lorentz local field correction factor, eq 3. The results for **1**−**7** are given in Table 1 (rows indicated as Lorentz). For the solvents studied here, $(n^2 + 2)/3$ varies from 1.26 to 1.42. Thus, gas-phase $[\alpha]_D$ values are increased by 26%−42%. The predicted ordering of $[\alpha]_D$ values is that of $(n^2 + 2)/3$, namely, $CH_3OH < CH_3CN < (CH_3)_2CO < C_6H_{12} < CHCl_3 < CCl_4 < C_6H_6$, independent of the solute molecule. Since the ordering of experimental $[\alpha]_D$ values varies substantially with the solute molecule, and, for the molecules **1**−**7**, in no case exhibits the ordering of the solvent $(n^2 + 2)/3$ values, it is clear that eq 3 does not correctly describe the variation in $[\alpha]_D$ with solvent. In Figures 4 and 5, we compare the predicted changes in $[\alpha]_D$ from C_6H_{12} to $(CH_3)_2CO$, CH_3OH, and CH_3CN and to CCl_4, C_6H_6, and $CHCl_3$ respectively, with the experimental changes. The correlation is very poor for both groups of solvents. Overall, the variations predicted using eq 3 are much smaller than the observed variations.

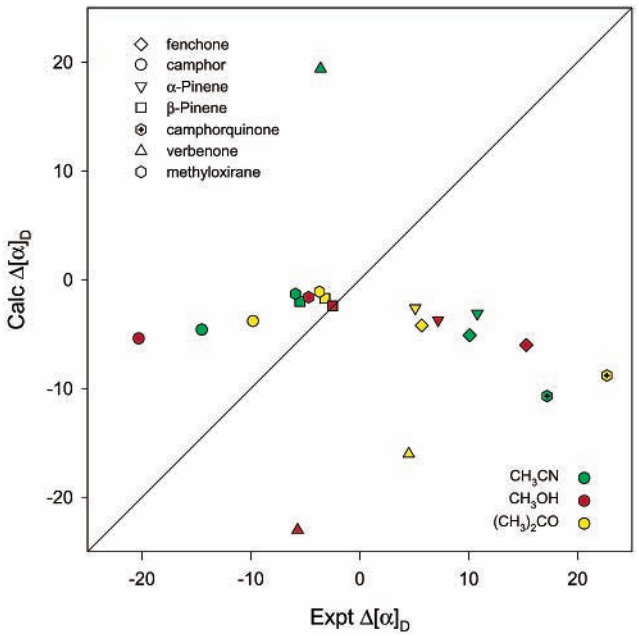

Figure 4. Comparison of variations in experimental $[\alpha]_D$ values for **1**−**7** in $(CH_3)_2CO$, CH_3OH, and CH_3CN, $\Delta[\alpha]_D$, to values calculated using gas-phase DFT $[\alpha]_D$ values and the Lorentz local field correction factor (eq 3). The line is of slope +1.

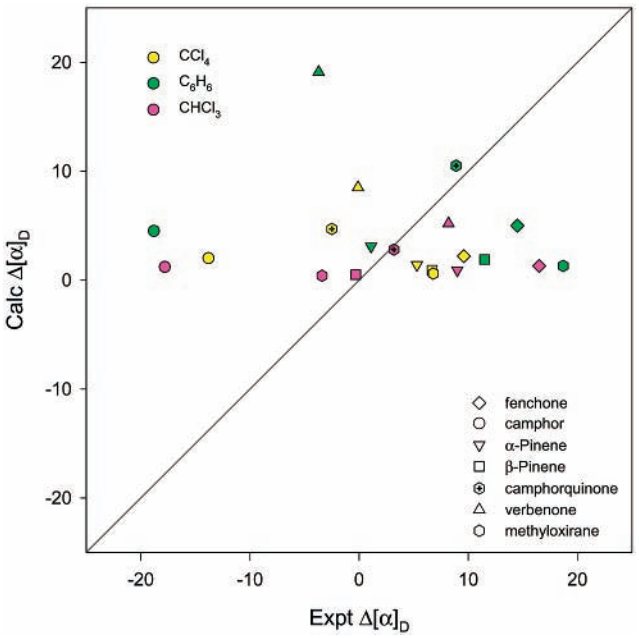

Figure 5. Comparison of variations in experimental $[\alpha]_D$ values for **1**−**7** in CCl_4, C_6H_6, and $CHCl_3$, $\Delta[\alpha]_D$, to values calculated using gas-phase DFT $[\alpha]_D$ values and the Lorentz local field correction factor (eq 3). The line is of slope +1.

Discussion

We have applied the state-of-the-art IEF-PCM methodology to the prediction of solvent effects on optical rotations using DFT. Our work constitutes an extension of prior applications of the PCM to solvent effects on frequency-dependent molecular polarizabilities and magnetic properties.[9]

DFT/nonequilibrium PCM calculations of $[\alpha]_D$ for seven molecules successfully predict variations in $[\alpha]_D$ for the solvents C_6H_{12}, $(CH_3)_2CO$, CH_3OH, and CH_3CN; for the solvents CCl_4, C_6H_6, and $CHCl_3$, DFT/PCM calculations are much less successful. The IEF-PCM is an electrostatic model. We therefore infer that for the solvents $(CH_3)_2CO$, CH_3OH, and CH_3CN

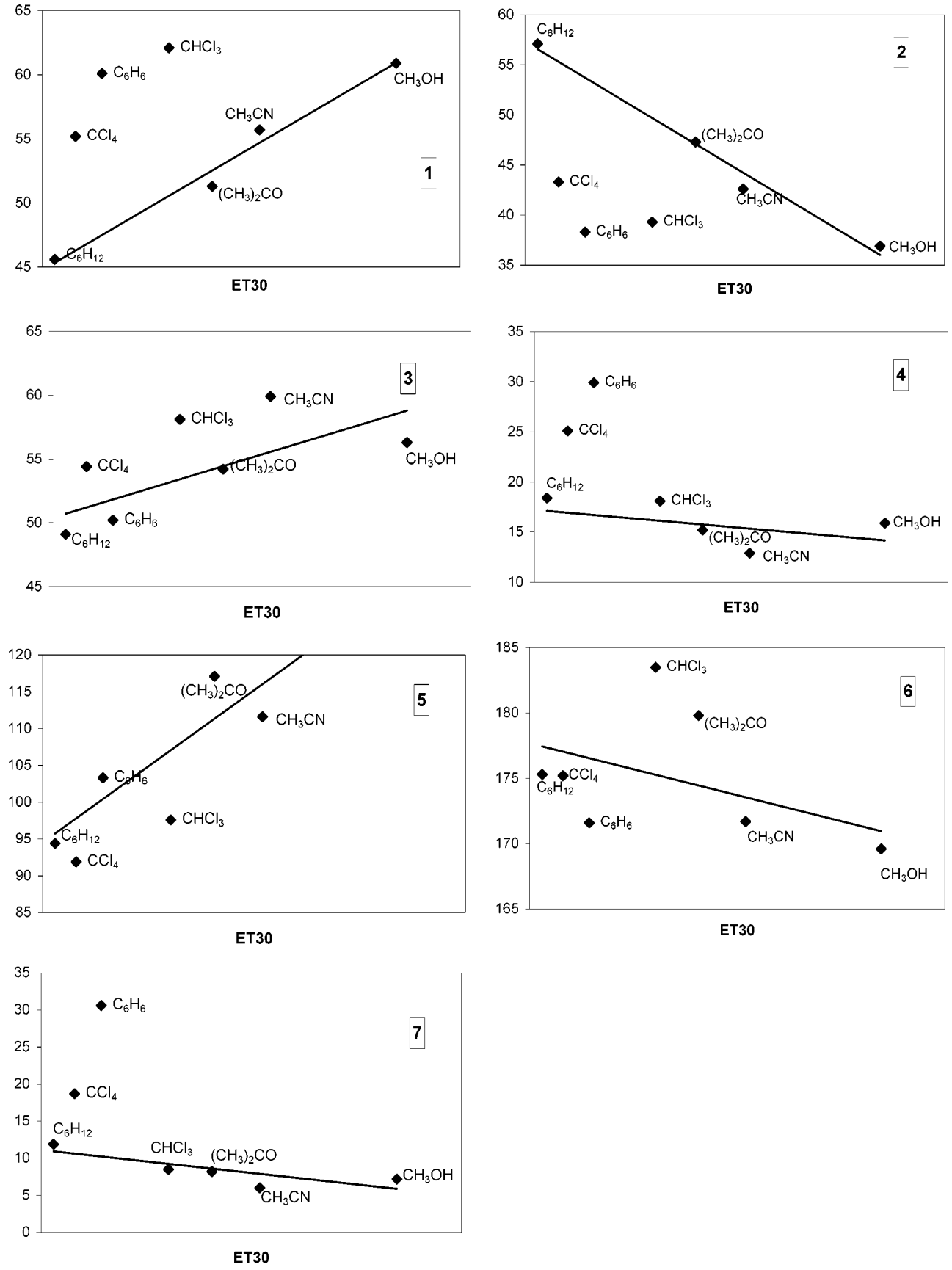

Figure 6. Comparison of experimental $[\alpha]_D$ values for **1**−**7** with respect to solvent ET30 values. ET30 values are as follows: C_6H_{12}, 30.9; CCl_4, 32.4; C_6H_6, 34.3; $CHCl_3$, 39.1; $(CH_3)_2CO$, 42.2; CH_3CN, 45.6; CH_3OH, 55.4. In the plots, we also report the lines obtained with a best fitting procedure on the C_6H_{12}, $(CH_3)_2CO$, CH_3CN, and CH_3OH values.

variations in $[\alpha]_D$ are predominantly electrostatic in origin while for CCl_4, C_6H_6, and $CHCl_3$ this is not the case. Support for this analysis is provided by plots of $[\alpha]_D$ versus the solvent polarity parameter ET30, which is derived from the solvatochromic effect of a solvent on the electronic absorption of the dye, pyridinium-*N*-phenoxide betaine.[20] As seen in Figure 6, for all seven molecules **1**−**7**, $[\alpha]_D$ values for C_6H_{12}, $(CH_3)_2CO$, CH_3OH, and CH_3CN vary approximately linearly with ET30 while $[\alpha]_D$ values for CCl_4, C_6H_6, and $CHCl_3$ deviate substantially from linearity. This finding is not unprecedented.[21]

The excellent agreement of DFT/PCM and experimental variations in $[\alpha]_D$ for C_6H_{12}, $(CH_3)_2CO$, CH_3OH, and CH_3CN is contingent on the use of the nonequilibrium PCM. Calculations using the equilibrium PCM are in poor agreement with experiment. It is clear that the nonequilibrium model is physically more appropriate. It is gratifying that it is simultaneously in better agreement with experiment.

The IEF-PCM calculations discussed above have not included the cavity-field correction (the second term in eq 17). For one molecule, **2**, we have carried out dynamic/nonequilibrium DFT/PCM calculations in which the cavity-field contribution is included with the results given in Table 1 (row indicated as dyn/neq/lf). The absolute magnitude of $[\alpha]_D$ increases uniformly by ~10% on inclusion of the cavity-field correction; the changes in $[\alpha]_D$ with variation of solvent are very little affected. The quality of the agreement between the DFT/PCM calculations and experiment is essentially unmodified.

Our work constitutes a major advance in the treatment of solvent effects on optical rotations. While there have been many experimental studies of solvent effects on optical rotations since the 1930s, they have been universally analyzed using eqs 1−3. Indeed, a molecular parameter Ω', termed "the molecular rotivity", has been defined by[1]

$$\Omega' = \frac{\alpha}{(n_s^2 + 2)/3} \tag{41}$$

to correct experimental specific rotations for the "local-field" effect, and solvent effect studies have frequently focused on the variation in Ω' with solvent (see, for example, ref 2). The usefulness of Ω' rests, of course, on the validity of the Lorentz expression for γ_{LF} (eq 3). The continued use of eqs 1−3 is quite surprising, given the recognition as long ago as the 1930s of the serious deficiencies of the Lorentz treatment of the local field. The classic work of Onsager, which introduced the concept of the reaction field and constituted an enormous step forward in understanding solvent (dielectric) effects was published in 1936.[22] Despite the widespread application of Onsager's work and its further development, notably by Kirkwood, for reasons which are entirely unclear, eqs 1−3 have remained unchallenged until now, with the notable exception of the single paper of Applequist,[23] in which solvent effects on the optical rotation of CHFClBr were predicted using an atom dipole interaction model for optical rotation and a spherical cavity continuum dielectric solvent model. One could hypothesize that to some extent this stasis has originated in the fact that, until recently, useful first principles calculations of optical rotations have been beyond the power of quantum chemists. However, even the recent papers in which ab initio Hartree−Fock methods have been used to calculate optical rotations have continued to use eqs 1−3, including solvent effects via eq 3.[8a−8l] The major deficiencies of this approach to including solvent effects have been made clear empirically by our DFT calculations for 28 rigid organic molecules.[3] Using B3LYP and the aug-cc-pVDZ basis set, the mean absolute deviation of calculated $[\alpha]_D$ values from experimental values was 23.1° when solvent effects were totally ignored ($\gamma_{LF} = 1$). When eq 3 was used to include solvent effects, the deviation increased to 54.0°. The results reported here further document the erroneous predictions of solvent effects arrived at when eqs 1−3 are used. Both qualitatively and quantitatively, for the seven solvents studied, predicted solvent effects are in very poor agreement with experiment. It is clear that continued use of this approach to the prediction of solvent effects on optical rotations is neither theoretically nor experimentally supportable.

The conclusions reached above are based on a relatively small set of molecules and solvents. Studies on a much larger range of molecules and solvents are required to confirm the reliability of our conclusions. In addition, it would be of great interest to include optical rotation measurements under solvent-free conditions (i.e., in the gas phase) in future studies. Gas-phase values of $[\alpha]_D$ for **1**−**7** are not currently available, and consequently, it has not been possible in this work to compare calculated and experimental absolute solvent effects. Instead, we have been limited to comparisons of calculated and experimental changes in $[\alpha]_D$ from one solvent to another. Recent developments in polarimetric instrumentation, specifically the application of cavity ring down techniques to the measurement of optical rotation, have enhanced the sensitivity of polarimetric instrumentation and facilitated measurements on gases at low pressures.[24] Such measurements, in combination with measurements in solutions, will permit the reliability of DFT/PCM calculations to be assessed more definitively.

As implemented here, the IEF-PCM includes only electrostatic solute−solvent interactions. We have concluded that for some solvents this is a serious limitation. The inclusion of nonelectrostatic effects is therefore important if a larger range of solvents is to be treated successfully. Nonelectrostatic effects, including dispersion and repulsion interactions, have previously been incorporated into the framework of the PCM to compute electric response properties,[25] but extensions to the calculation of optical rotations have not been formulated yet; further studies in this direction are surely required.

Conclusion

There is an enormous body of literature relating to the quantitative prediction of solvent effects on molecular properties. However, since the formulation of the quantum mechanical theory of optical rotation, when solvent effects were included via the Lorentz local-field approximation, the treatment of solvent effects on the optical rotations of chiral molecules has been virtually ignored. Our work brings to bear on this problem a state-of-the-art methodology for treating solvent effects: the IEF-PCM. The IEF-PCM approach to solvent effects is combined with the most accurate quantum-mechanical technique currently available for the calculation of the electric dipole−magnetic dipole polarizability, $\beta_{\alpha\beta}(\nu)$, which uses DFT. Together, the combination of DFT and IEF-PCM permits, for the first time, calculations of solvent effects on optical rotation in which solute−solvent interactions are explicitly included.

The $[\alpha]_D$ values of the seven chiral molecules, **1**−**7**, that we have studied exhibit widely varying solvent effects in the seven chosen solvents. We have shown that, for some solvents, DFT/PCM calculations predict variations in $[\alpha]_D$ in excellent agreement with experiment. For other solvents, agreement is poor. Within the PCM, solute−solvent interactions are entirely electrostatic in nature. We therefore conclude that the quality of the agreement between DFT/PCM and experimental solvent

variations in $[\alpha]_D$ reflects the degree to which solute−solvent interactions are in fact purely electrostatic. For the molecules studied, the solvent effects in C_6H_{12}, $(CH_3)_2CO$, CH_3OH, and CH_3CN are found to be predominantly electrostatic; in C_6H_6, CCl_4, and $CHCl_3$, the opposite is found to be the case.

Thus, our general conclusions are that (1) the DFT/PCM methodology reliably models the electrostatic contributions to solvent effects on optical rotations and (2) the importance of electrostatic contributions to solvent effects on optical rotations, relative to other contributions, varies considerably with the nature of the solvent.

Acknowledgment. One of us (P.J.S.) is grateful to the National Science Foundation for financial support (Grant CHE-9902832). B.M and J.T are grateful to the Italian CNR (through Agenzia 2000 project) for financial support.

References and Notes

(1) Eliel, E. L.; Wilen, S. H. *Stereochemistry of Organic Compounds*; Wiley: New York, 1994; Chapter 13.

(2) Kumata, Y.; Furukawa, J.; Fueno, T. *Bull. Chem. Soc. Jpn.* **1970**, *43*, 3920.

(3) Stephens, P. J.; Devlin, F. J.; Cheeseman, J. R.; Frisch, M. J. *J. Phys. Chem. A* **2001**, *105*, 5356.

(4) (a) Cancès, E.; Mennucci, B. *J. Math. Chem*. **1998**, *23*, 309. (b) Cancès, E.; Mennucci, B.; Tomasi, J. *J. Chem. Phys*. **1997**, *107*, 3032. (c) Mennucci, B.; Cancès, E.; Tomasi, J. *J. Phys. Chem. B* **1997**, *101*, 10506.

(5) (a) Miertus, S.; Scrocco, E.; Tomasi, J. *Chem. Phys*. **1981**, *55*, 117. (b) Cammi, R.; Tomasi, J. *J. Comput. Chem.* **1995**, *16*, 1449.

(6) (a) Rosenfeld, L. *Z. Phys.* **1928**, *52*, 161. (b) Condon, E. U. *Rev. Mod. Phys.* **1937**, *9*, 432. (c) Eyring, H.; Walter, J.; Kimball, G. E. *Quantum Chemistry*; Wiley: New York, 1944; Chapter XVII, p 342.

(7) Lorentz, H. A. *The Theory of Electrons*; Teubner: Leipzig, Germany, 1916; p 305 (reprinted by Dover: New York, 1951).

(8) (a) Polavarapu, P. L. *Mol. Phys.* **1997**, *91*, 551. (b) Polavarapu, P. L. *Tetrahedron: Asymmetry* **1997**, *8*, 3397. (c) Polavarapu, P. L.; Chakraborty, D. K. *J. Am. Chem. Soc*. **1998**, *120*, 6160. (d) Polavarapu, P. L.; Zhao, C. *Chem. Phys. Lett.* **1998**, *296*, 105. (e) Polavarapu, P. L.; Chakraborty, D. K. *Chem. Phys*. **1999**, *240*, 1. (f) Polavarapu, P. L.; Zhao, C. *J. Am. Chem. Soc*. **1999**, *121*, 246. (g) Polavarapu, P. L.; Chakraborty, D. K.; Ruud K. *Chem. Phys. Lett.* **2000**, *319*, 595. (h) Kondru, R. K.; Wipf, P.; Beratan, D. N. *J. Am. Chem. Soc*. **1998**, *120*, 2204. (i) Kondru, R. K.; Wipf, P.; Beratan, D. N. *Science* **1998**, *282*, 2247. (j) Kondru, R. K.; Wipf, P.; Beratan, D. N. *J. Phys. Chem. A* **1999**, *103*, 6603. (k) Kondru, R. K.; Chen, C. H.; Curran, D. P.; Beratan, D. N.; Wipf, P. *Tetrahedron: Asymmetry* **1999**, *10*, 4143. (l) Ribe, S.; Kondru, R. K.; Beratan, D. N.; Wipf, P. *J. Am. Chem. Soc*. **2000**, *122*, 4608. (m) Pericou-Cayere, M.; Rerat, M.; Dargelos, A. *Chem Phys*. **1998**, *226*, 297. (n) Yabana, K.; Bertsch, G. F. *Phys. Rev. A* **1999**, *160*, 127. (o) Cheeseman, J. R.; Frisch, M. J.; Devlin, F. J.; Stephens, P. J. *J. Phys. Chem. A* **2000**, *104*, 1039. (p) Stephens, P. J.; Devlin, F. J.; Cheeseman, J. R.; Frisch, M. J.; Mennucci, B.; Tomasi, J. *Tetrahedron: Asymmetry* **2000**, *11*, 2443. (q) Stephens, P. J.; Devlin, F. J.; Cheeseman, J. R.; Frisch, M. J. *Chirality* **2002**, *14*, 288. (r) Grimme, S. *Chem. Phys. Lett.* **2001**, *339*, 380. References n−r contain DFT calculations of optical rotation.

(9) For recent applications of the PCM to molecular properties, see, for example: (a) Cammi, R. *J. Chem. Phys*. **1998**, *109*, 3185. (b) Cammi, R.; Mennucci, B.; Tomasi, J. *J. Am. Chem. Soc*. **1998**, *120*, 8834. (c) Cammi, R.; Mennucci, B.; Tomasi, J. *J. Phys. Chem. A* **1998**, *102*, 870. (d) Cammi, R.; Mennucci, B.; Tomasi, J. *J. Chem. Phys*. **1999**, *110*, 7627. (e) Mennucci, B.; Cammi, R.; Tomasi, J. *Int. J. Quantum Chem*. **1999**, *75*, 767. (f) Tomasi, J.; Cammi, R.; Mennucci, B. *Int. J. Quantum Chem*. **1999**, *75*, 783. (g) Cammi, R.; Mennucci, B.; Tomasi, J. *J. Phys. Chem. A* **2000**, *104*, 4690. (h) Mennucci, B.; Martinez, J., Tomasi, J. *J. Phys. Chem. A* **2001**, *105*, 7287.

(10) See, for example: Jorgensen, P.; Simons, J. *Second Quantization-Based Methods In Quantum Chemistry* Academic Press: New York, 1981 for a review on SCF/MCSCF/CC response theory and Autschbach, J.; Ziegler, T. *J. Chem. Phys.* **2002**, 116, 891 for DFT.

(11) Amos, R. D. *Chem. Phys. Lett*. **1982**, *87*, 23.

(12) (a) London, F. J. *Phys. Radium* **1937**, *8*, 397. (b) Ditchfield, R. *Mol. Phys.* **1974**, *27*, 789.

(13) Johnson, B. G.; Frisch, M. J. *J. Chem. Phys*. **1994**, *100*, 7429.

(14) McWeeny, R. *Methods of Molecular Quantum Mechanics*, 2nd ed.; Academic Press: London, 1992; Chapter 12.

(15) (a) Feyereisen, M.; Nichols, J.; Oddershede, J.; Simons, J. *J. Chem. Phys*. **1992**, *96*, 2978. (b) Rice, J. E.; Amos, R. D.; Coldwell, S. M.; Handy, N. C.; Sanz, J. *J. Chem. Phys*. **1990**, *93*, 8828. (c) Weiss, H.; Ahlrichs, R.; Haser, M. *J. Chem. Phys*. **1993**, *99*, 1262.

(16) For a general discussion on solving CP equations, see: (a) Frisch, M. J.; Head-Gordon, M.; Pople, J. A. *Chem. Phys*. **1990**, *141*, 189. (b) Pople, J. A.; Krishnan, R.; Schlegel, H. B.; Binkley, J. S. *Int. J. Quantum Chem. Symp.* **1979** *13*, 325.

(17) Cammi, R.; Mennucci, B. *J. Chem. Phys*. **1999**, *110*, 9877.

(18) (a) Aguilar, M. A.; Olivares del Valle, F. J.; Tomasi, J. *J. Chem. Phys*. **1993**, *98*, 7375. (b) Cammi, R.; Tomasi, J. *Int. J. Quantum Chem.: Quantum Chem. Symp*. **1995**, *29*, 465. (c) Mennucci, B.; Cammi, R.; Tomasi, J. *J. Chem. Phys*. **1998**, *109*, 2798. (d) Cappelli, C.; Corni, S.; Cammi, R.; Mennucci, B.; Tomasi, J. *J. Chem. Phys*. **2000**, *113*, 11270.

(19) Frisch, M. J.; Trucks, G. W.; Schlegel, H. B.; Scuseria, G. E.; Robb, M. A.; Cheeseman, J. R.; Zakrzewski, V. G.; Montgomery, J. A., Jr.; Stratmann, R. E.; Burant, J. C.; Dapprich, S.; Millam, J. M.; Daniels, A. D.; Kudin, K. N.; Strain, M. C.; Farkas, O.; Tomasi, J.; Barone, V.; Cossi, M.; Cammi, R.; Mennucci, B.; Pomelli, C.; Adamo, C.; Clifford, S.; Ochterski, J.; Petersson, G. A.; Ayala, P. Y.; Cui, Q.; Morokuma, K.; Malick, D. K.; Rabuck, A. D.; Raghavachari, K.; Foresman, J. B.; Ortiz, J. V.; Baboul, A. G.; Cioslowski, J.; Stefanov, B. B.; Liu, G.; Liashenko, A.; Piskorz, P.; Komaromi, I.; Gomperts, R.; Martin, R. L.; Fox, D. J.; Keith, T.; Al-Laham, M. A.; Peng, C. Y.; Nanayakkara, A.; Challacombe, M.; Gill, P. M. W.; Johnson, B.; Chen, W.; Wong, M. W.; Andres, J. L.; Gonzalez, C.; Head-Gordon, M.; Replogle, E. S.; Pople, J. A. *Gaussian 99*, development version; Gaussian, Inc.: Pittsburgh, PA, 1999.

(20) Reichardt, C. *Solvents and Solvent Effects in Organic Chemistry*; VCH: Weinheim, Germany, 1990; and references therein.

(21) See, for example: (a) Wiberg, K. B.; Keith, T. A.; Frisch, M. J.; Murcko, M. *J. Phys. Chem*. **1995**, *99*, 9072. (b) Wiberg, K. B.; Rablen, P. R.; Rush, D. J.; Keith, T. A *J. Am. Chem. Soc*. **1995**, *117*, 4261 and references therein.

(22) Onsager, L. *J. Am. Chem. Soc*. **1936**, *58*, 1486.

(23) Applequist, J. *J. Phys. Chem*. **1990**, *94*, 6564.

(24) Müller, T.; Wiberg, K. B.; Vaccaro, P. H. *J. Phys. Chem*. A **2000**, *104*, 5959.

(25) Mennucci, B.; Amovilli, C.; Tomasi, J. *Chem. Phys. Lett*. **1998**, *286*, 221.